

# Curved layer path planning on a 5-axis 3D printer

Joao Duarte, Isabel Espirito Santo, M. Teresa T. Monteiro and A. Ismael F. Vaz  
ALGORITMI Research Centre, University of Minho, Guimaraes, Portugal

## Abstract

**Purpose** – This paper aims to provide an approach to print shell-type objects using a 5-axis printer. The proposed approach takes advantage of the two additional printer degrees of freedom to provide a curved layer path planning strategy.

**Design/methodology/approach** – This paper addresses curved layer path planning on a 5-axis printer. This printer considers movements along the three usual axes together with two additional axes at the printing table (rotation and tilt), allowing to build more complex and reliable objects. Curved layer path planning is considered where polygons obtained from the slicing stage are approximated by linear and cubic splines. The proposed printing strategy consists in building an inner core supporting structure followed by outer curved layers.

**Findings** – The curved layer path planning strategy is validated for shell-type objects by considering a 5-axis printer simulator. An example with an aeronautic object is presented to illustrate the proposed approach.

**Originality/value** – The paper presents an approach to curved layer path planning on a 5-axis printer, for shell-type objects.

**Keywords** 3D, Additive manufacturing, Curved layer, Splines, 3D printing, Curved path planning

**Paper type** Research paper

## 1. Introduction

In the past decades, additive manufacturing (AM) has increased its impact and importance in the society due to its applications in several industrial areas such as aeronautics and automobile. AM may also allow to reduce the energy consumption and environment impact by efficient use of material. Extensive literature about AM has been produced during the past three decades further confirming its importance in the society.

In the AM process, and according to Kulkarni *et al.* (2000), path is the trajectory followed by the machine nozzle, either if it is depositing, curing or cutting. A suitable planning of the nozzle path can bring benefits to the geometry being manufactured, concerning quality and building time. Quality and building time of the final product can be affected by the deposition rate, layer height, push-out time, suck-back time and the diameter of the nozzle tip (Melgoza *et al.*, 2014). This led to the development of different strategies such as raster, zigzag, contour, spiral, fractal space curves, hybrid, medial axis transformation (MAT), direction-parallel and more recently curved layer.

According to Kulkarni *et al.* (2000) path planning includes determining the geometry/topology of the paths, computing the paths and determining the appropriate process parameters. Path planning may comprise two components: the interior and the exterior path. In the interior planning, geometric path and the process parameters associated with the path are determined, while the exterior path planning controls the accuracy of the external geometry (Kulkarni *et al.*, 2000). Usually external path

planning consists in material removal, including techniques such as milling, cutting, lasers and water jet laser.

An accurate path planning becomes therefore essential, since it can allow to avoid discontinuities between the filaments deposition. Accurate path planning will lead to a strength improvement between layers by increasing void-free and gap-free depositions, resulting in an increased quality of the built objects (Ding *et al.*, 2015; Ding *et al.*, 2016). For example, according to Jin *et al.* (2017b), two of the major causes of the unevenness of the deposited surface are the sharp corners and the non-uniform spacing between adjacent paths. The application of an adequate strategy for the process of the path planning optimization can therefore result in an improvement of the deposition quality, efficiency and in the decrease of time traveled by the machine nozzle.

The importance given to the path planning stage on the AM process is well documented in literature, where different strategies to determine the optimal path have been addressed. Regardless of the strategy used, the main goal becomes the quality improvement of the geometries being manufactured using the least possible time. For example, in Wojcik *et al.* (2017) a comparative analysis between zigzag, contour, spiral and fractal strategies is made to access the efficiency of all types of algorithms. Results show that an algorithm based on the zigzag strategy turns up to be better than the other approaches.

---

This work was developed under the FIBR3D project Hybrid processes based on additive manufacturing of composites with long or short fibers reinforced thermoplastic matrix (POCI-01-0145-FEDER-016414), supported by the Lisbon Regional Operational Programme 2020, under the PORTUGAL 2020 Partnership Agreement, through the European Regional Development Fund (ERDF).

Received 3 February 2021

Revised 29 June 2021

10 September 2021

Accepted 13 September 2021

---

The current issue and full text archive of this journal is available on Emerald Insight at: <https://www.emerald.com/insight/1355-2546.htm>



Rapid Prototyping Journal  
© Emerald Publishing Limited [ISSN 1355-2546]  
[DOI 10.1108/RPJ-02-2021-0025]

Several path planning strategies for standard 3 degree of freedom printers have been proposed, like the ones based on a non-uniform rational basis spline curve (Jin *et al.*, 2013), a divide and conquer strategy (Ding *et al.*, 2014), a layer-by-layer approach (Melgoza *et al.*, 2014), an adaptive path planning using the MAT algorithm (Ding *et al.*, 2016) and a fractal based tool-path for area filling (Kapil *et al.*, 2016).

Recently, a new strategy named curved layered fused deposition modelling has emerged. The difference for the flat layered is that, in flat layered, the model is printed in a two-dimensional platform. In curved layered printing, no flat surface is used allowing to decrease the number of layers and, consequently, decreasing the staircase effect. According to Huang and Singamneni (2015), the curved layer slicing starts with the selection of a surface as the original model surface. During building, the filaments will be deposited along curved layers instead of planar layers. This result is a substantial improvement of the mechanical properties of the objects compared with the traditional horizontal path strategies (Chakraborty *et al.*, 2008). For example, in Chakraborty *et al.* (2008) a curved layered fused deposition model for path generation is presented, Lim *et al.* (2016) developed a curved-layered printing path using an environment called Grasshopper, a plugin of Rhinoceros[[copyright](#)], Song *et al.* (2017) considers a slight curved deposition path, and Patel *et al.* (2015) define curved layer as a new strategy for the manufacturing of curved, thin and shell-type geometries and uneven surfaces.

Deposition along curved layers allows to obtain better material structure and object strength because of the fiber continuity, reduction of the stair stepping effect and the reduction of the number of layers (Guan *et al.*, 2015). According to Jin *et al.* (2017a), in the curved layer fused deposition, the normal vector of the surface at the deposition points is always changing. Therefore, during the deposition, the ideal is to ensure that the extrusion head is always perpendicular to the geometry surface. The best way to ensure this is considering the use of a 5-axis printer, having in mind that it may lead to a reduction of economy and simplicity of the system.

More recently in Xu *et al.* (2019), authors consider a complex object decomposition, by using a geometric algorithm, to avoid the need of supports when printing in a 3 + 2-axis printer. Another decomposition approach for multi-axis printing can be found in Dai *et al.* (2018). In Chen *et al.* (2019), authors present an algorithm for thin-shells using a multi-axis printer and curved layer slicing. Allen and Trask (2015) presented a new strategy for curved layer fused deposition using a delta robot and the CURA [[copyright](#)] software for the generation of the path. In Allen and Trask (2015), the curved layer path is obtained by dividing the geometry model in two parts: the core and the skin of the geometry. The core is the first part being built, working as support and for process simplification.

Here, a five degrees of freedom 3D printer that considers a hybrid process based on additive manufacturing of composites with long or short fibers-reinforced thermoplastic matrix is being considered under the FIBR3D project. The printer has the three (along  $x$ ,  $y$  and  $z$ ) standard degrees of freedom and two additional degrees of freedom consisting in the possibility to rotate and tilt the printer bed. Five actuators are used to provide the five degrees of freedom leading to a 5-axis printer. While the majority of previous works address curved layer path

planning in standard 3D printers (by using a non flat surface), we are interested in taking advantage of the five degrees of freedom printer to provide a new path planning technique. Therefore, this paper main contribution is the proposal of a curved layer path planning strategy for shell-type objects. The provided strategy allows different deposition directions as requested by some fiber-reinforced objects. Since the printer is still under testing a simulator is used to validate the proposed strategy.

The paper addresses the curved layer path planning in Section 2, where we introduce the reader to the printer characteristics, type of objects we are interested in and to splines (linear and cubic). We describe how the path is generated in Section 3, by making use of an illustrative example of the proposed approach and we conclude in Section 4.

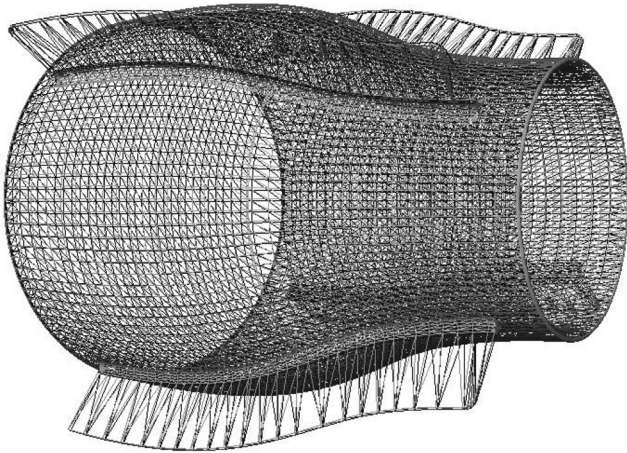
## 2. Curved layer manufacturing

Typically, four stages can be considered in the printing process: object optimal orientation (Pereira *et al.*, 2018), support generation, slicing and path planning. In the slicing stage, standard 3D printers consider slices of the object to be printed, along the slicing direction. Usually the slicing direction corresponds to a direction along the  $z$  axis and each slice corresponds to a given  $z$  axis layer. The object is printed by addressing each layer consecutively, with each layer being built with movements on the  $x$ ,  $y$  axes. So, movement on the  $z$  axis is typically restricted to change the printing layer.

The present work considers a five degrees of freedom printer where curved layer manufacturing is not restricted to the  $x$ ,  $y$  and  $z$  axes, taking advantage of the two additional degrees of freedom to build more complex objects with higher quality. The two additional degrees of freedom are located at the printer table, allowing it to tilt with respect to the  $y$  axis and rotate with respect to the  $z$  axis. The printer considers a (unique) nozzle and was developed to deposit composite material with long or short fibers of reinforced thermoplastic matrix. This work focus on the path planning stage, where we further assume that the object is already optimal oriented, there is no need of supports, and fixed height slicing is to be performed. Additionally, we assume that deposition occurs at a constant speed, i.e. path planning does not need to consider additional parameters during the path planning stage. These assumptions makes this a conceptual strategy that can be used in the context of dynamic height slicing (as long as adaptive height deposition is possible) and with any type of material (provided that enough adhesiveness properties are present).

While the herein proposed strategy to curved layer manufacturing may be applied to several types of objects or materials, we are majorly interested in building objects with applications in the aerospace industry, namely, objects of shell type like the one presented in Figure 1. A deposition path that takes advantage of the five degrees of freedom printer is to be computed. Deposition takes place with the printer head following the object (facets) normal direction or perpendicularly to the object normal direction, so we can minimize the staircase effect resulting from the additive manufacturing process.

The herein proposed technique prints first the core of the structure by using a classical slicing approach (i.e. slicing with planes normal to the  $z$  axis) and the remaining object is printed using curved layers, working like a coat on this core.

**Figure 1** Example of an aeronautic shell-type object

The next section provides the 5-axis printer computer-aided design (CAD) route for printing. The standard slicing process (intersecting a  $z$  plane with the object facets) is used to generate a set of polygons that describe (in a 2D form) the object layers. These polygons are to be approximated by splines and Section 2.2 is dedicated to set our notation. The splines are later on used to produce the object core, with planar layers, and the remaining object, with curved layers. Bed table orientation (tilt and rotation) is described in Section 2.3.

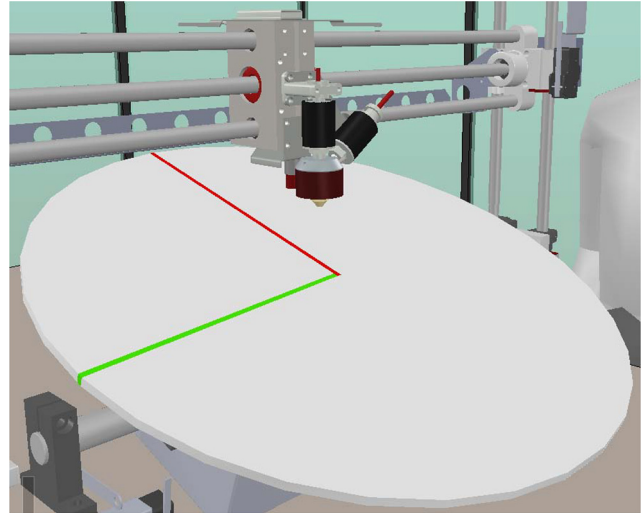
### 2.1 Computer-aided design route

Typically one uses a favorite CAD software to design the object and export it in a standard triangle language or standard tessellation language (STL) file format. For 3-axis printers, there are several available (slicing) software that inputs the object in a STL file format and provides the necessary G-Code to control the printer (e.g. Slic3r ([The Slic3r project, 2021](#)) or CURA [copyright] ([Ultimaker Cura software, 2021](#))). The STL file format contains a description of the 3D object to be printed, which consists in a set of facets (triangles defined by three points/vertices) and corresponding normal directions (pointing to the object exterior). Slicing software usually provides a number of pre-configured 3D 3-axis printer models and generates a set of control instruction (e.g. temperature settings) for the selected printer, together with the path where material deposition takes place.

A virtual representation of the 5-axis the printer considered in this work is presented in [Figure 2](#) [see FIBR3DEmul ([Faria et al., 2020](#)) for additional details]. The emulator and the 5-axis printer use the same CAD route to obtain the G-Code. Available software for 3-axis 3D printing can also be used for this printer, but it takes no advantage on the extra degrees of freedom available at the printer table.

### 2.2 Path planning using splines

While the herein proposed approach is devoted to curved layer path planning, our settings are somehow different to the ones already addressed in the literature. Our printer provides a flat printing bed, so curved layer path planning is related to build layers that may not be perpendicular to the  $z$  axis. While conventional slicing is to take place to obtain 2D polygons describing the object, advantage of interpolation by splines is taken to provide a virtual representation

**Figure 2** 5-axis printer virtual representation

of the object. Splines are then used to build the object core, with layers perpendicular to the  $z$  axis, and the remaining object using curved layers, which may not be perpendicular to the  $z$  axis.

#### 2.2.1 Splines

A spline is a unidimensional piecewise interpolating function defined by segments between knots (interpolation points used to define the spline). Splines are characterized by their simplicity in the definition and easiness to compute and evaluation. These properties make them appealing for our application. While each segment used between two consecutive knots can theoretically be any (continuous) function, the one with greater interest are polynomials of degree one or three. Linear polynomials are more simple to compute and evaluate, but, in general, it makes the spline non-differentiable at the knots. Cubic polynomials are used when smoothness and interpolation of first and second derivatives are requested, at the expense of solving a linear system of equations to determine the spline coefficients. When segments are first order polynomials (linear functions) we have a linear spline. When segments are polynomials of degree three we have a cubic spline. For this application splines with linear and cubic segments are considered, depending on the accuracy requested and the shape of the polygons to be interpolated.

Let  $t_i$ ,  $i = 0, \dots, n$ ,  $t_i < t_{i+1}$ , and  $f_i = f(t_i)$  be a set of knots and corresponding function values, respectively. A spline is a parametric function depending on the  $t$  parameter (often representing the time) and used to interpolate the function  $f$  at the given set of  $n + 1$  knots is composed of  $n$  segments, each one defined by two consecutive knots. A spline in its general form is given by:

$$s_d(t) = \begin{cases} s_d^1(t) & t \in [t_0, t_1] \\ s_d^2(t) & t \in [t_1, t_2] \\ \dots & \\ s_d^n(t) & t \in [t_{n-1}, t_n], \end{cases} \quad (1)$$

where  $s_d^i(t)$ ,  $i = 1, \dots, n$ , are the linear ( $d = 1$ ) or cubic ( $d = 3$ ) segments. The spline is well defined if we have  $n \geq 2$  for a linear spline and  $n \geq 3$  for a cubic spline.



Linear segments between two knots are easy to compute and are defined by:  $s_1^i(t) = f_{i-1} + \frac{f_i - f_{i-1}}{t_i - t_{i-1}}(t - t_{i-1})$ ,  $i = 1, \dots, n$ . Cubic segments are defined by:

$$s_3^i(t) = \frac{M_{i-1}}{6(t_i - t_{i-1})}(t_i - t)^3 + \frac{M_i}{6(t_i - t_{i-1})}(t - t_{i-1})^3 \\ + \left[ \frac{f_{i-1}}{t_i - t_{i-1}} - \frac{M_{i-1}(t_i - t_{i-1})}{6} \right] (t_i - t) \\ + \left[ \frac{f_i}{t_i - t_{i-1}} - \frac{M_i(t_i - t_{i-1})}{6} \right] (t - t_{i-1})$$

with coefficients  $M_i$ ,  $i = 1, \dots, n$ , computed by solving a linear system of equations where interpolation conditions of the function and continuity are imposed. End conditions are also imposed to obtain a feasible (full rank) linear system. See, e.g. Boor (2001), for additional readings about splines.

### 2.2.2 Splines to interpolate polygons

Uniform slicing is considered along the  $z$  coordinate, i.e. slicing takes place at the horizontal plane  $z = z^\ell$ ,  $\ell = 1, \dots, L$ , where  $L$  is the number of slicing layers. After slicing along the  $z$  coordinate we are left with 2D closed polygons representing the object layers. Each polygon is defined by a set of linear segments resulting from the intersection of a plane with the facets. Let  $(x_i^\ell, y_i^\ell)$ ,  $i = 0, \dots, n^\ell$ , represent a set of points defining a polygon, for a given  $\ell$  layer. Each polygon is then interpolated by two parametric splines. One interpolates the  $x$  coordinate and other the  $y$  coordinate, i.e. we have a 2D polygon represented as the parametric function

$$P^\ell(t) = (x^\ell(t), y^\ell(t)), \quad (2)$$

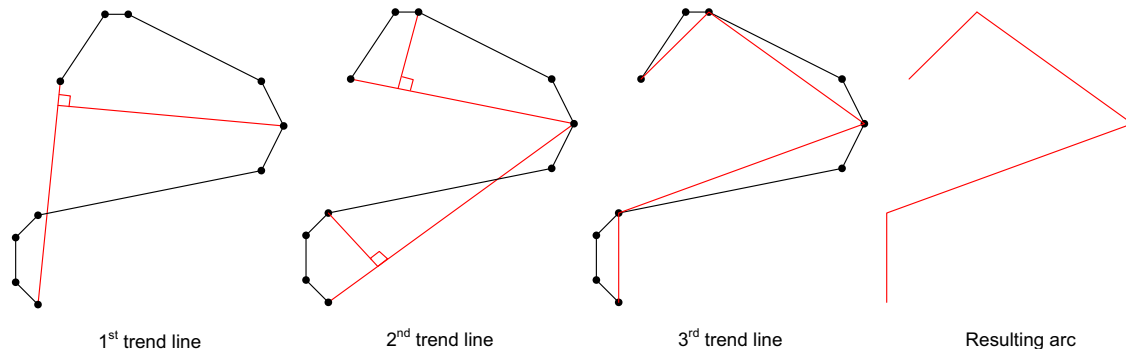
with  $x^\ell(t) = s_x^\ell(t)$  and  $y^\ell(t) = s_y^\ell(t)$ ,  $t \in [t_0^\ell, t_{n^\ell}^\ell]$ .

From the interpolation conditions we have  $P^\ell(t_i^\ell) = (x^\ell(t_i^\ell), y^\ell(t_i^\ell)) = (x_i^\ell, y_i^\ell)$ ,  $i = 0, \dots, n^\ell$ ,  $\ell = 1, \dots, L$ .

Assuming the nozzle moves at the same speed in both  $x$  and  $y$  axis, we consider  $t$  to represent the time step proportional to the Euclidean distance, and we take, without loss of generality,  $t_0^\ell = t_0 = 0$  and  $t_i^\ell = \|(x_i^\ell, y_i^\ell) - (x_{i-1}^\ell, y_{i-1}^\ell)\|_2$ ,  $i = 1, \dots, n^\ell$ .

For shell-type objects we obtain two 2D polygons per layer, defining the exterior and interior of the object. We further extend our notation in (2) to denote  $P_{in}^\ell(t)$  and  $P_{out}^\ell(t)$  as the interior and exterior parametric curves that interpolate the polygons, respectively.

**Figure 3** Example of the Douglas and Peucker (1973) algorithm



### 2.2.3 Reducing the number of knots

Slicing along the  $z$  coordinate may lead to polygons with a huge number of segments, in special if we have curved objects with high curvature defined by a high number of facets. Since polygons are to be interpolated by splines, a significant number of points may be dropped, as long as the spline continues to provide acceptable accuracy for printing. E.g. consecutive segments with (almost) the same slope may be defined by a single segment. Please note that this reduction in the number of points does not have a direct consequence on the printing time but may lead to smaller G-Code file size.

The Douglas–Peucker algorithm (Douglas and Peucker, 1973) aims a segmented line simplification by keeping critical points (associated with the splines knots), maintaining the essential shape of the original segmented line. The algorithm starts by considering a trend line between the end points of the segmented line (Figure 3). It then checks if the distance of the remaining points to the trend line are within a given tolerance. The algorithm stops if the maximum distance between the trend line and all remain points is within a given tolerance, since the trend line approximates the segmented line to the given tolerance. Otherwise the algorithm proceeds recursively by considering the trend lines defined by the current end points and the point that attains the maximum distance to the current trend line.

Since we are interested in applying the Douglas–Peucker algorithm to a closed polygon, it needs to be adapted for the case of the given segmented line starts and ends at the same point. In such a case we simple proceed recursively by taking the two segmented lines formed by the end points and the central point in the polygon. The pseudo code is presented in Algorithm 1 and Figure 4 illustrates an example. The algorithm controls the accuracy between the initial and the final polygons by considering a given  $\epsilon$  tolerance.

**Algorithm 1** Douglas–Peucker Adapted Algorithm (DPAA)

1: **procedure** DPAA

**Input:**  $(x_i, y_i)$ ,  $i = 0, \dots, n$ ,  $n > 1$ .  $\epsilon > 0$ .

**Output:** A set  $\mathcal{L}$  of points defining a segmented line.

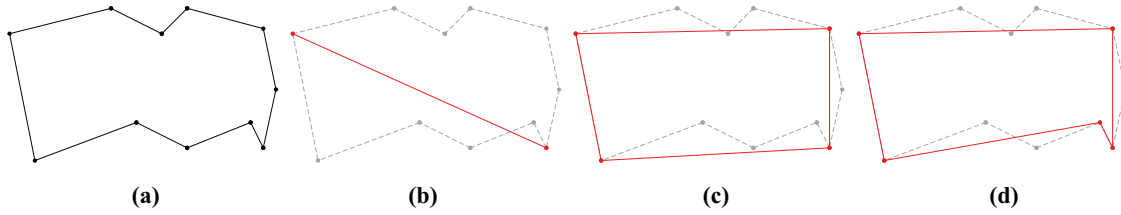
2: **if**  $n == 2$  **then**

**return**  $\mathcal{L} = \{(x_0, y_0), (x_1, y_1)\}$ .

3: **if**  $(x_0, y_0) == (x_n, y_n)$  **then**

4:  $\mathcal{L} = DPAA(\{(x_0, y_0), \dots, (x_{\lfloor n/2 \rfloor}, y_{\lfloor n/2 \rfloor})\}) \cup DPAA(\{(x_{\lfloor n/2 \rfloor}, y_{\lfloor n/2 \rfloor}), \dots, (x_n, y_n)\})$ .

**return**  $\mathcal{L}$ .

**Figure 4** Douglas–Peucker Adapted Algorithm example

**Notes:** (a) The input polygon; (b) the initial start and end points; (c) simplified polygon after first round; (d) final simplified polygon

- 5: Let  $d$  be the maximum distance from the line segment  $(x_0, y_0)(x_n, y_n)$  to all points  $(x_i, y_i), i = 1, \dots, n-1$ , and  $i_d$  the index of a point at a distance  $d$  to the line segment.
- 6: **if**  $d < \epsilon$  **then**  
return  $\mathcal{L} = \{(x_0, y_0), (x_n, y_n)\}$ .
- 7: **else**  
return  $\mathcal{L} = DPAA(\{(x_0, y_0), \dots, (x_{i_d}, y_{i_d})\}) \cup DPAA(\{(x_{i_d}, y_{i_d}), \dots, (x_n, y_n)\})$ .

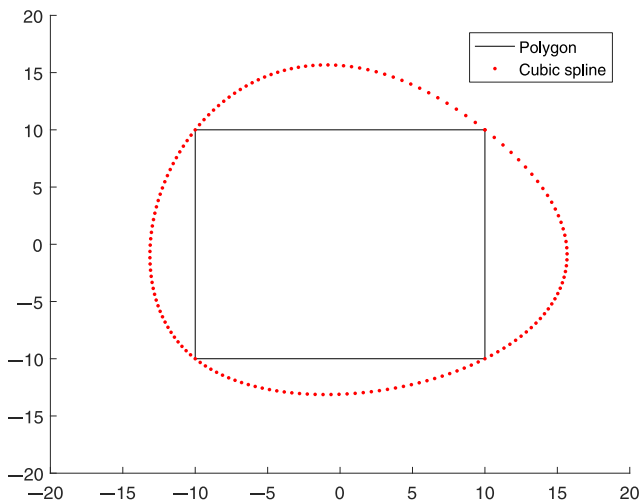
#### 2.2.4 Linear and cubic mixed splines

The segments of splines defined by (1) are usually of one type: either linear or cubic ( $d = 1$  or  $d = 3, \forall i = 1, \dots, n$ ). However, fixing the same polynomial degree of all segments may lead to a bad approximation of the polygon. E.g., cubic splines may provide a bad approximation when the angle between two consecutive segments is *big* (see an example in Figure 5, where a squared polygon is approximated by a cubic spline).

To avoid an undesirable behavior in the approximation we build the spline by allowing segments to be linear or cubic polynomials, depending on the smoothness of the polygon to be interpolated. Our spline is, therefore, defined as

$$s(t) = s_{d^i}^i(t), \quad t \in [t_{i-1}, t_i], \quad \forall i \in \{1, \dots, n\},$$

where  $d^i$  is the polynomial degree for each segment  $i = 1, \dots, n$ .

**Figure 5** Interpolation of a square using a cubic spline

The decision about getting a linear or cubic segment is made based on the angle formed by two consecutive line segments, i.e. if  $\Theta = \arccos\left(\frac{\vec{u}_i \cdot \vec{u}_{i+1}}{\|\vec{u}_i\| \|\vec{u}_{i+1}\|}\right)$ , where  $\vec{u}_i = (x_{i+1}, y_{i+1}) - (x_i, y_i), i = 1, \dots, n-2$ , is bigger than a specified tolerance  $tol$ , then the segment  $i$  is part of a linear spline (Figure 6). A linear segment is considered when  $n \leq 2$ , since a cubic segment requests at least  $n \geq 3$  points to be built. Figure 6 illustrates an example where the first two segments are linear polynomials while the last three form a cubic polynomial segment.

#### 2.3 Bed table orientation

For curved layer path planning the nozzle orientation (or equivalently, bed table orientation) is also important to control, since deposition needs to be made along the object facets normal or perpendicular (to the normal) direction. The normal and its perpendicular directions can be obtained during the slicing process. The line segment obtained from the intersection of the facet with the slicing plane is used to compute the normal perpendicular direction (Figure 7). Depending on the printing stage the printing direction uses the facet perpendicular normal direction (e.g. for the object core) or the facet normal direction (e.g. for the remaining object). For the herein 5-axis printer setting, the nozzle orientation is aligned with the printing direction by moving the printer table (tilt and rotate), which is not possible in a standard 3-axis printer.

### 3. Generating the paths

In this section we put together all the machinery described in the previous sections applied to an example. A workflow for the curved layer path planning is presented in Algorithm 2.

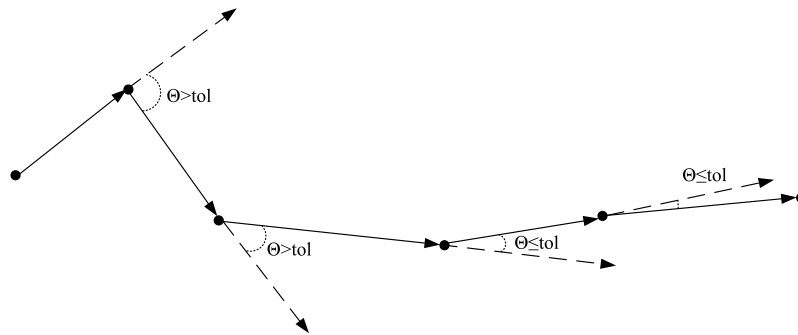
**Algorithm 2** Main steps of the curved layer path planning workflow.

#### 1: procedure MAIN PROCEDURE

**Input:** STL file describing the object.

**Output:** G-Code file with curved layer path planning.

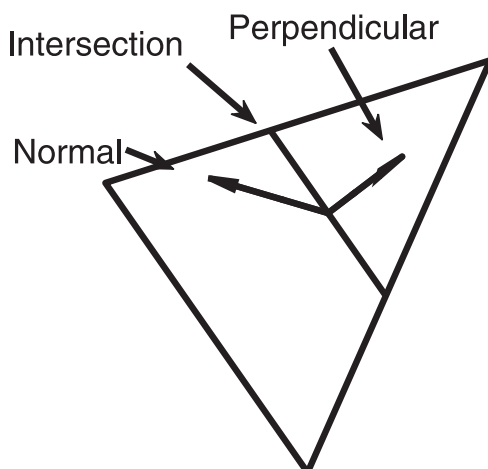
- 2: Read the STL file.
- 3: Optimal object orientation (Pereira et al., 2018).
- 4: Use a standard slicing strategy to obtain inner and outer polygons.
- 5: Compute  $P_{in}^\ell(t)$  and  $P_{out}^\ell(t), \ell = 1, \dots, L$ .
- 6: Generate G-Code to control the printer (e.g. control temperature, home positioning, brim, core support).

**Figure 6** Selection between linear or cubic polynomial segments of a spline

- 7: Generate G-Code to build the object core (using replications of  $P_{in}^{\ell}(t)$ ).
- 8: **while** replications of  $P_{in}^{\ell}(t)$  do not reach  $P_{out}^{\ell}(t)$ ,  $\ell = 1, \dots, L$  **do**
- 9:     **for**  $t = 0$  to  $max_{\ell=1, \dots, L} t_{nt}^{\ell}$  with a fixed step size (e.g. the nozzle thickness) **do**
- 10:         Generate the G-Code for the curved layer path with the replication of  $P_{in}^{\ell}(t)$ ,  $\ell = 1, \dots, L$ .
- 11:         **for**  $\ell = 1, \dots, L$  **do**
- 12:             Generate the G-Code for the curved layer path with the replication of  $P_{in}^{\ell}(t)$ ,  $t \in t_{nt}^{\ell}$
- 13:     Generate G-Code to control the printer (e.g. control temperature, retracting home)

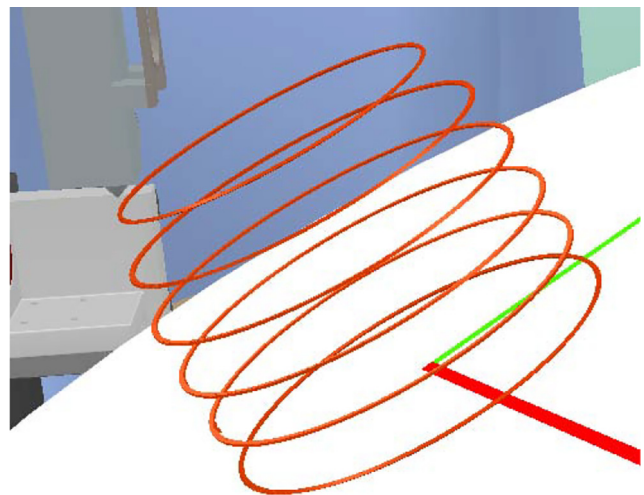
After an optimal part orientation (Pereira et al., 2018) we proceed with a fixed step slicing along the  $z$  axis (intersecting equidistant  $z$  planes with the object facets), building layers of polygons that describe the object. For shell-type parts (the ones we are interested in) inner and outer polygons are obtained, which are then interpolated by using splines, getting  $P_{in}^{\ell}(t)$  and  $P_{out}^{\ell}(t)$ ,  $\ell = 1, \dots, L$  (Steps 4 and 5 in Algorithm 2).

The path planning strategy for shell-type parts starts to produce the object core, made of three replications of the inner polygons ( $P_{in}^{\ell}(t)$ ) per object layer (from  $t = 0$  to  $t = t_{nt}^{\ell}$ ,  $\ell = 1, \dots, L$ ), defining the core thickness (Step 7 in Algorithm 2). Printing the three inner polygons replications is made in layers perpendicular to the  $z$ -axis. These layers are printed

**Figure 7** Object facet normal and its perpendicular directions

using the normal perpendicular direction of the facets, which may request the printer table to be tilted. While three replications were used in the present work to define the core thickness, any number of replications can be used in order to obtain an initial structure (core) that can support the remaining curved layers (depending on the deposition material used). Figure 8 presents a print screen from the FIBR3DEmul (Faria et al., 2020) simulator when building the core of the object. While a slicing height of 0.4 mm is being considered, the simulation only presents one slice for each  $40 \times 0.4 = 1.6$  cm, for better visibility. In the picture, each circumference is made by three depositions of the inner polygon replications, i.e. it provides circumferences with a height of 0.4 mm and a thickness of 1.2 mm.

Remaining curved layers, to be built on top of the core, are obtained by taking the inner polygon  $P_{in}^{\ell}(t)$ , adding the nozzle thickness to the spline knots along the facet normal direction (i.e. replicating the inner polygons), until the outer polygon  $P_{out}^{\ell}(t)$  is reached. Curved layers are built by alternating between a deposition along a path generated by fixing a  $t$  value for each

**Figure 8** Printing of the object core

**Notes:** Each layer is made of three replications of the inner polygons, defining the core  
 J\_ID: RPJ ART NO: 10.  
 1108/RPJ-02-2021-0025 Date: 28-September-21 Page: 6 Total  
 Pages: 9 4/Color Figure(s) ARTTYPE="ResearchArticle" ID:  
 Sjs

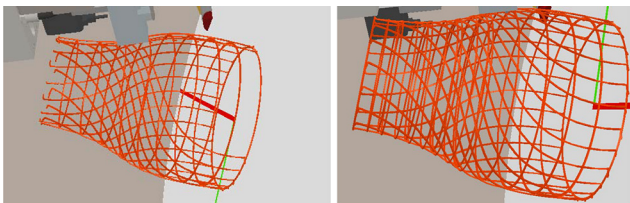
layer  $\ell$  (from  $\ell = 1, \dots, L$  for fixed  $t$  values in  $[0, \max_{\ell=1, \dots, L} t_{n^\ell}^\ell]$  – step 10) and a deposition following a path similar to the one used to build the core, i.e. fixing  $\ell$  and taking  $t \in [0, t_{n^\ell}^\ell]$  (step 13). Both deposition curved layer strategies consider the facet normal direction to compute the table tilt. The (first) deposition, obtained by fixing  $t$ , provides a curved layer along the core layers, which is then crossed with the second deposition.

Figure 9 depicts the deposition of the remaining object, after printing the object core. The figure on the left presents the deposition of the first curved layer, done after printing the object core. The core is represented by the circumferences and the curved layer is being built on top of it with curved movements. This curved layer is achieved by considering paths for a fixed  $t$  value using  $P_{in}^\ell(t)$  plus three times the nozzle thickness (since the core was built by considering three replication of the polygons), for  $\ell = 1, \dots, L$ , with the printer head aligned with the facet normal direction. The figure on the right presents the second curved layer, made on top of the first curved layer. This layer is achieved by considering paths for a fixed  $\ell$  value using  $P_{in}^\ell(t)$  plus four times the nozzle thickness, for  $t \in [0, \max_{\ell=1, \dots, L} t_{n^\ell}^\ell]$ . This second curved layer deposition is similar to the one used for the core. While the core layers deposition uses the printer head aligned with the facet normal perpendicular direction, this second curved layer deposition takes place considering the facet normal direction. This deposition strategy will provide pairs of layers with different deposition orientations, as requested by fiber made objects. Other deposition strategy can be used. For example, the selection of the  $t$  value may be done so that pairs of layers are crossed with a selected angle between depositions, with a possible increase in the part robustness and quality, or by selecting a different combination of curved layers type.

The object is fully printed by printing combinations of curved layers, using inner polygons replications, until the outer polygons are reached, i.e. replications of  $P_{in}^\ell(t)$  are intersected with  $P_{out}^\ell(t)$  to find regions of the object where deposition is to take place. Therefore, the shell object grid fins are also printed using the proposed strategy and they can be observed in Figure 10.

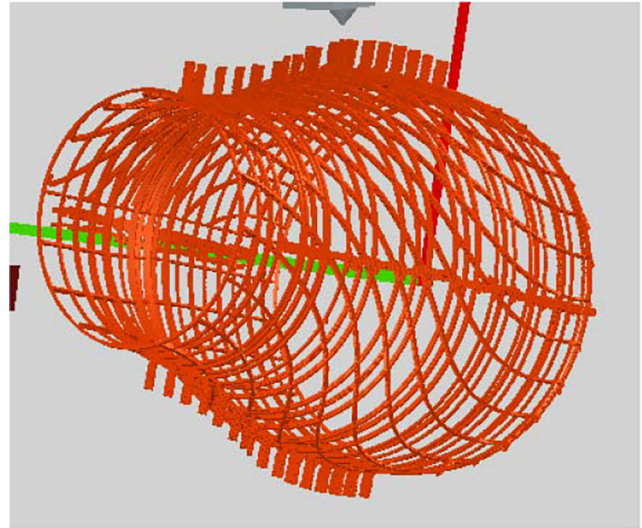
While the FIBR3DEmul is able to detect collisions between the printer components (head, table and remaining hardware) this was not considered herein for the sake of simplicity. However, a supporting structure can be built by printing additional layers in the core consisting in repeating the first layer of the object until enough distance from the printer table is attained (in this case a support of 10 cm would be enough). A

**Figure 9** Printing of the object outer layers



**Notes:** On the left the first curved layer (after the core built) and on the right the second curved layer

**Figure 10** Final printing of the object outer layers (grid fins)



retract command (taking the  $z$  axis to a safe position) is also needed when the core is finished, to avoid a collision (between the printer head and the already deposited material) when a change in the deposition strategy is taken.

Algorithm 2 is implemented in the FIBR3DApp software, which can be obtained from the last author or visiting the GitHub FIBR3DApp project. While the current implementation only uses G01 G-Code commands, which is a direct translation between the splines sampled points to G-Code, G02 and G03 commands could be used to approximate the cubic splines segments.

## 4. Conclusions

A curved layer path planning strategy for a five degrees of freedom printer for additive manufacturing of composites with long or short fibers is proposed. This path planning strategy considers the traditional CAD route, where objects are provided to the printer driver software in the STL file format. While the traditional slicing is being used, the novelty comes with the representation of the obtained polygons by linear and cubic splines and a strategy to print complex shell-type objects using curved layers. The use of splines allows curved layer deposition following the normal facets direction or the normal perpendicular direction, taking advantage on the printer ability to tilt and rotate the printer table. The strategy for shell-type objects consists in building an object core followed by curved layers (possible crossed) depositions, suitable for fiber-type objects. Deposition along the facets normal perpendicular direction may also allow the minimization of the staircase effect in complex 3D objects. While no study about the total printing time was made, the herein proposed strategy is likely to lead to a large printing time, due to the need to change between different layers deposition strategies. An application is provided for a shell-type object from aeronautics, illustrating the usefulness of the proposed strategy. A implementation of the proposed strategy can be obtained at the GitHub FIBR3DApp project.



## References

- Allen, R.J.A. and Trask, R.S. (2015), "An experimental demonstration of effective curved layer fused filament fabrication utilising a parallel deposition robot", *Additive Manufacturing*, Vol. 8, pp. 78-87.
- Boor, C.D. (2001), *A Practical Guide to Splines*, rev. ed., Applied mathematical sciences, Springer, Berlin.
- Chakraborty, D., Aneesh Reddy, B. and Choudhury, A.R. (2008), "Extruder path generation for curved layer fused deposition modeling", *Computer-Aided Design*, Vol. 40 No. 2, pp. 235-243.
- Chen, L., Chung, M.-F., Tian, Y., Joneja, A. and Tang, K. (2019), "Variable-depth curved layer fused deposition modeling of thin-shells", *Robotics and Computer-Integrated Manufacturing*, Vol. 57, pp. 422-434.
- Dai, C., Wang, C.C.L., Wu, C., Lefebvre, S., Fang, G. and Liu, Y.-J. (2018), "Support-free volume printing by multi-axis motion", *ACM Transactions on Graphics*, Vol. 37 No. 4, pp. 134:1-134:14.
- Ding, D., Pan, Z.(S.), Cuiuri, D. and Li, H. (2014), "A tool-path generation strategy for wire and arc additive manufacturing", *The International Journal of Advanced Manufacturing Technology*, Vol. 73 Nos 1/4, pp. 173-183.
- Ding, D., Pan, Z., Cuiuri, D. and Li, H. (2015), "A practical path planning methodology for wire and arc additive manufacturing of thin-walled structures", *Robotics and Computer-Integrated Manufacturing*, Vol. 34, pp. 8-19.
- Ding, D., Pan, Z., Cuiuri, D., Li, H. and Larkin, N. (2016), "Adaptive path planning for wire-feed additive manufacturing using medial axis transformation", *Journal of Cleaner Production*, Vol. 133, pp. 942-952.
- Douglas, D.H. and Peucker, T.K. (1973), "Algorithms for the reduction of the number of points required to represent a digitized line or its caricature", *Cartographica: The International Journal for Geographic Information and Geovisualization*, Vol. 10 No. 2, pp. 112-122.
- Faria, C., Fonseca, J. and Bicho, E. (2020), "FIBR3DEmul – an open-access simulation solution for 3D printing processes of FDM machines with 3+ actuated axes", *The International Journal of Advanced Manufacturing Technology*, Vol. 106 Nos 7/8, pp. 3609-3623.
- Guan, H.W., Savalani, M.M., Gibson, I. and Diegel, O. (2015), "Influence of fill gap on flexural strength of parts fabricated by curved layer fused deposition modeling", *Procedia Technology*, Vol. 20, pp. 243-248.
- Huang, B. and Singamneni, S. (2015), "Curved layer adaptive slicing (CLAS) for fused deposition modelling", *Rapid Prototyping Journal*, Vol. 21 No. 4, pp. 354-367.
- Jin, Y.A., He, Y. and Fu, J.Z. (2013), "An adaptive tool path generation for fused deposition modeling", *Advanced Materials Research*, Vol. 819, pp. 7-12.
- Jin, Y., Du, J., He, Y. and Fu, G. (2017a), "Modeling and process planning for curved layer fused deposition", *The International Journal of Advanced Manufacturing Technology*, Vol. 91 Nos 1/4, pp. 273-285.
- Jin, Y., Du, J., Ma, Z., Liu, A. and He, Y. (2017b), "An optimization approach for path planning of high-quality and uniform additive manufacturing", *The International Journal of Advanced Manufacturing Technology*, Vol. 92 Nos 1/4, pp. 1-12.
- Kapil, S., Joshi, P., Vithasth Yagani, H., Rana, D., Kulkarni, P. M., Kumar, R. and Karunakaran, K.P. (2016), "Optimal space filling for additive manufacturing", *Rapid Prototyping Journal*, Vol. 22 No. 4, pp. 660-675.
- Kulkarni, P., Marsan, A. and Dutta, D. (2000), "A review of process planning techniques in layered manufacturing", *Rapid Prototyping Journal*, Vol. 6 No. 1, pp. 18-35.
- Lim, S., Buswell, R.A., Valentine, P.J., Piker, D., Austin, S.A. and De Kestelier, X. (2016), "Modelling curved-layered printing paths for fabricating large-scale construction components", *Additive Manufacturing*, Vol. 12 No. Part B, pp. 216-230.
- Melgoza, E.L., Vallicrosa, G., Serenó, L., Ciurana, J. and Rodríguez, C.A. (2014), "Rapid tooling using 3d printing system for manufacturing of customized tracheal stent", *Rapid Prototyping Journal*, Vol. 20 No. 1, pp. 2-12.
- Patel, Y., Kshattriya, A., Singamneni, S.B. and Roy Choudhury, A. (2015), "Application of curved layer manufacturing for preservation of randomly located minute critical surface features in rapid prototyping", *Rapid Prototyping Journal*, Vol. 21 No. 6, pp. 725-734.
- Pereira, S., Vaz, A.I.F. and Vicente, L.N. (2018), "On the optimal object orientation in additive manufacturing", *The International Journal of Advanced Manufacturing Technology*, Vol. 98 Nos 5/8, pp. 1685-1694.
- Song, H., Ray, N., Sokolov, D. and Lefebvre, S. (2017), "Anti-aliasing for fused filament deposition", *Computer-Aided Design*, Vol. 89, pp. 25-34.
- The Slic3r project (2021), "Slic3r", available at: [slic3r.org](http://slic3r.org)
- Ultimaker Cura software (2021), "CURA", available at: [ultimaker.com/en/products/ultimaker-cura-software](http://ultimaker.com/en/products/ultimaker-cura-software)
- Wojcik, M., Pozniak-Koszalka, I., Koszalka, L. and Kasprzak, A. (2017), "Experimentation system for path planning applied to 3d printing", in Duffy, V.G. (Ed.), *Advances in Applied Digital Human Modeling and Simulation: Proceedings of the AHFE 2016 International Conference on Digital Human Modeling and Simulation, July 27-31, 2016, Walt Disney World [Copyright], FL*, Springer International Publishing, Cham, pp. 291-302.
- Xu, K., Chen, L. and Tang, K. (2019), "Support-free layered process planning toward 3 + 2-axis additive manufacturing", *IEEE Transactions on Automation Science and Engineering*, Vol. 16 No. 2, pp. 838-850.

## Corresponding author

A. Ismael F. Vaz can be contacted at: [aivaz@dps.uminho.pt](mailto:aivaz@dps.uminho.pt)